

High Energy Nuclear Collisions: Theory Overview

R J Fries

Cyclotron Institute and Department of Physics and Astronomy, Texas A&M University, College Station TX 77845, USA

and RIKEN/BNL Research Center, Brookhaven National Laboratory, Upton NY 11973, USA

Abstract. We review some basic concepts of Relativistic Heavy Ion Physics and discuss our understanding of some key results from the experimental program at the Relativistic Heavy Ion Collider (RHIC). We focus in particular on the early time dynamics of nuclear collisions, some result from lattice QCD, hard probes and photons.

Keywords. Heavy Ion Collisions, Quark Gluon Plasma

PACS Nos XX

1. Introduction

The universe a few microseconds after the Big Bang was filled with a hot and dense phase of matter. We believe that quarks and gluon at those temperatures, above 10^{12} K, were deconfined and existed as a quark gluon plasma (QGP). These ideas can be tested in collisions of nuclei at ultra-relativistic energies. At the Relativistic Heavy Ion Collider (RHIC) nuclei as heavy as gold are accelerated to an energy of 100 GeV per nucleon. 40 TeV total energy is available in the collision of two of these nuclei. A large fraction of this energy is used to create new particles (a few thousand of them) and to give them kinetic energies. The energy in the collision is spread over a certain volume with peak energy densities of ~ 10 -30 GeV/fm³, much larger than in ordinary nuclear matter [1–3]. This process happens over a very short time (a few fm/c) but we have strong indications from observables like elliptic flow v_2 that despite the short life times thermalization of the matter is reached. The peak energy densities are safely above the predicted critical energy densities ≈ 1 GeV/fm³ for a phase transition from hadrons to a quark gluon plasma [4].

In the first decade of RHIC a large amount of experimental results has been gathered. Some results have confirmed expectations, like jet quenching. Others have turned out to be more difficult to decipher, e.g. signals from quarkonia that promised to be simple plasma thermometers [5], yet others have been great surprises, like the indications for a perfect fluid created at RHIC. We do have firm evidence that we create equilibrated quark-gluon matter in the experiments at RHIC. [1,2,6]

In order to describe nuclear collisions at high energies and to filter out the properties of quark gluon plasma from the stream of experimental data we can slice the data in a simple way. Thermalization of particles does not extend beyond 2 GeV/c in transverse momentum

P_T around midrapidities, i.e. around 90° scattering angle from the beam axis. However, this includes 99% of all particles produced, the bulk of the collision. The tail of the hadron spectrum at high P_T does not come from thermalized matter but from QCD jets, yet it bears the imprint of the quark gluon plasma that the particles had to traverse in order to arrive at the detectors. It had already been realized in the 1980s that we can use high- P_T hadrons as “hard probes” of the quark gluon plasma phase [7].

In this overview we briefly cover some of the most fundamental approaches to heavy ion collisions from the theoretical side. We will discuss initial interactions and the color glass condensate, the current state of the lattice QCD results, jet quenching, and photons as an example for electromagnetic probes. We have to forgo some other very timely and important topics like heavy quarks, dileptons or hydrodynamics. The latter will be covered in an accompanying article by R. Bhalerao [8].

2. First Interactions

Interactions of hadrons or nuclei at small momentum transfers, below 1-2 GeV/c can not be described by standard perturbative QCD (pQCD) techniques. pQCD assumes rather dilute parton densities in the colliding hadrons and is valid at weak coupling. Experimental data show that the gluon distribution grows dramatically for larger energies (or small parton momentum fraction x) which must eventually lead to a breakdown of the standard pQCD picture. At very large energies the distribution of gluons in hadrons (and even more so in large nuclei) has to saturate, with gluon splittings and recombination happening in detailed balance. It has first been argued by McLerran and Venugopalan that in such a saturation scenario the gluon density $\sim Q_s^{-2}$ sets a new scale, the saturation scale, and that an effective theory can be constructed based on a quasi-classical approximation to QCD [9–11]. For $Q_s \gg \Lambda_{\text{QCD}}$ the coupling can still be weak, although the theory has non-trivial many-body effects included. This effective theory of QCD at very high collision energies, called the color glass condensate, describes a nuclear collision as the collision of two (highly Lorentz-contracted) sheets of color $SU(3)$ -charges [12,13].

The initial gluon fields A_1^μ, A_2^μ in the two nuclei before the collision are dominated by their *transverse* electric and magnetic components. After the collision, this creates extremely strong *longitudinal* (color-)electric and magnetic fields [14,15]

$$E_0 = ig[A_1^i, A_2^i], \quad B_0 = ig\epsilon^{ij}[A_1^i, A_2^j] \quad (1)$$

(expressed here in a suitable axial gauge), see Fig. 1. Note that the nuclei themselves (represented by the conserved net baryon number carried by the valence quarks) go through each other. Valence quarks (and other large- x partons) only scattering occasionally to create jets. The longitudinal fields expand in the space between the nuclei as they recede from each other. We now understand that these strong longitudinal fields are the means by which energy density is deposited in the center of the colliding system. The initial energy density is given by

$$\epsilon_0 = \frac{1}{2} (E_0^2 + B_0^2) \approx \frac{g^6 N_c (N_c^2 - 1)}{8\pi} \mu_1^2 \mu_2^2 \ln^2 \frac{Q^2}{\Lambda^2} \quad (2)$$

where the μ_i^2 are the densities of color charges in the two colliding nuclei and Q_0 and Λ are ultraviolet and infrared cutoffs.

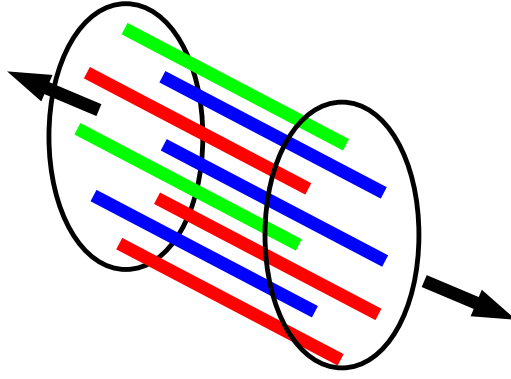


Figure 1. Two Lorentz-contracted nuclei shortly after the collision. The large momentum partons have gone through each other with small disturbance. Their gluon fields have interacted to form strong longitudinal fields which connect the receding nuclei and slow them down. The scenario is reminiscent of a “color” capacitor with moving plates.

The initial energy momentum tensor is diagonal with maximum pressure anisotropy. The “transverse pressure” — a slight abuse of terms so far from thermal equilibrium — is $p_T = T^{xx} = T^{yy} = \epsilon_0$ and the “longitudinal pressure” is $p_L = T^{zz} = -p_T = -\epsilon_0$. The negative longitudinal pressure corresponds to the fact that the fields slow down the sources and hence the nuclei themselves (similar to the electric field attracting two capacitor plates in electrodynamics). The strong longitudinal fields lead to the creation of transverse fields as time progresses and the anisotropy between transverse and longitudinal components of the energy momentum tensor decreases. Equilibration needs two important ingredients: the gluon field has to decohere into gluons and quark-antiquark pairs in order to make the longitudinal pressure positive, and eventually the pressure has to isotropize completely. The exact way in which thermalization into an equilibrated quark gluon plasma proceeds, at least within the very short time ($\lesssim 1$ fm/c) suggested by data, is unknown [16,17]. Plasma instabilities have recently been suggested as a possible mechanism [18,19]. The time for decoherence, a necessary ingredient for thermalization, was recently estimated to be proportional to $1/Q_s$ with a coefficient of order 1 [20,21]. For RHIC energies where Q_s is estimated to be in the range 1-2 GeV, decoherence times are thus consistent with the experimentally observed thermalization times. Once thermalization is reached, the expansion and cooling of quark gluon plasma is very well described by hydrodynamics. The strong longitudinal gluon fields could play an important role in two recent discoveries at RHIC: long-range rapidity correlations which could be a direct image of the elongated flux tubes [22], and parity violation from quarks interacting with topologically non-trivial gluon configurations associated with $\mathbf{E} \cdot \mathbf{B} \neq 0$ [23].

3. Lattice Estimates

In lattice QCD the partition function of QCD is evaluated on a discretized Euclidean space-time grid using Monte-Carlo techniques. Results have long confirmed our expectation, originally from considerations of asymptotic freedom, that quarks and gluons are decon-

fined at high temperatures and that chiral symmetry is restored. There are strong indications from realistic simulations of QCD with two light and one heavier quark flavors (for u , d , and s quarks resp.) that the phase transition is not of first order at vanishing net baryon densities, but a smooth cross over around a critical temperature T_c . Hence we do not expect a sharp transition, say of the energy density, but rather the thermodynamic properties change rapidly but smoothly as a function of temperature around T_c .

Lattice QCD at finite baryon chemical potential μ_B suffers from an unpleasant sign problem that makes Monte-Carlo techniques rather ineffective. In recent years, several techniques have been devised (reweighting, Taylor expansion around $\mu_B = 0$, etc.) to explore the phase diagram of QCD away from zero net baryon density. Most calculations agree that there is a critical point in a range $\mu_B \approx 200 \dots 400$ MeV from which on the cross over line between hadronic and quark gluon matter becomes a first order phase transition. Our understanding of the QCD phase diagram is shown schematically in Fig. 2.

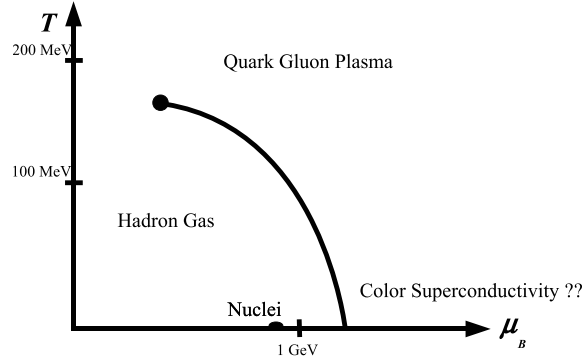


Figure 2. Schematic phase diagram of QCD. The first-order phase transition line ends in a critical point, at smaller baryon densities the transition between hadronic matter and quark gluon plasma is a cross over.

Many modern calculations use close to realistic light quark masses with pion masses as small as 200 MeV. Estimates for the critical temperature at small baryon densities — the domain in which RHIC at top energies and the Large Hadron Collider (LHC) are operating — range from 176 to 192 MeV [24,25]. This is a rather large discrepancy for results from different groups. While many results hint at one common temperature for the chiral and deconfinement phase transition, one group sees evidence for a chiral transition at 151 MeV while they measure the deconfinement transition at 176 MeV [24]. The divergence of predictions has recently attracted a lot of attention and is under investigation.

There is however consensus on the gross features of the QCD equation of state calculated on the lattice. Around the critical temperature the normalized energy density ϵ/T^4 exhibits a large jump due to the drastic increase in degrees of freedom going from the hadronic phase (basically pions below T_c) to the deconfined phase with quarks and gluons. ϵ/T^4 and the reduced pressure p/T^4 do not reach their Stefan-Boltzmann limit even around $4 \times T_c$ which has been interpreted as a hint for the strongly interacting nature of quark gluon plasma even far above the phase transition [4]. However, refined perturbative calculations can describe the lattice results reasonably well down to about $2 \times T_c$ [26].

More recently it has been attempted to extract transport coefficients like the shear vis-

cosity η and the bulk viscosity β of quark gluon plasma from lattice QCD calculations. As improved viscous relativistic hydrodynamic calculations become more and more available the interest in these new observables will increase [8].

4. Hard Probes

Jet quenching, the loss of high momentum particles in nuclear collisions had long been predicted theoretically [7]. When it was finally observed in early RHIC data the effect turned out to be very large. Nearly 80% of the particles expected at a given transverse momentum P_T were suppressed in central collisions of gold nuclei. We quantify this suppression most conveniently by the nuclear modification factor

$$R_{AA} = \frac{dN^{AA}/P_T}{\langle N_{\text{coll}} \rangle dN^{pp}/dP_T} \quad (3)$$

which is the ratio of particle yields in nucleus-nucleus vs proton-proton collisions modulo the number of binary collisions expected in a nuclear collision. For a loose superposition of nucleon collision the modification factor would be (close to) unity. In fact there are a few “cold” nuclear matter effects which lead to deviations of R_{AA} from unity. These include modifications of parton distributions for nucleons bound in nuclei vs free nucleons (known as shadowing and the EMC effect), and multiple scattering in the initial state which leads to the so-called Cronin effect [27]. At top RHIC energies we expect particles produced with a few GeV energy around midrapidity to exhibit anti-shadowing, i.e. a slight enhancement, which gives way to a suppression at larger P_T . The Cronin effect leads to an enhancement for the same particles at a few GeV which dies out toward higher P_T . However, all of these cold nuclear matter effects are small, and partially competing with each other. In summary they lead to deviations of R_{AA} from unity of less than 20%.

Two effects are important to understand the energy loss of a fast quark or gluon propagating through quark gluon plasma. First, the dominating mechanism for energy loss, at least for light quarks and gluons, is through induced gluon radiation. This leads to larger suppression than energy loss than from elastic collisions. Secondly, the dependence of the energy loss on the path length L is quadratic, $\Delta E \propto L^2$. This LPM effect (after Landau, Pomeranchuk and Migdal who first described the similar effect in quantum electrodynamics [28,29]) comes from a destructive interference. Consider a parton radiating a gluon with energy ω and relative transverse momentum k_T . The formation time of the parton-gluon system is given by $\tau_f = \omega/k_T^2$, and further radiation during this time is suppressed. In other words, if the mean free path λ of the parton is smaller than the typical formation time ω/k_T^2 , then the scattering off $N_{\text{coh}} = \tau_f/\lambda$ number of partons happens coherently. This leads to a differential energy loss $dE/dx = -\hat{q}x$ per unit path length, and to the famous quadratic path dependence of the total energy loss. The transport coefficient \hat{q} parameterizes the momentum transfer between the medium and the parton. It is given by the momentum transfer squared μ^2 per mean free path,

$$\hat{q} = \frac{\mu^2}{\lambda}. \quad (4)$$

Comparisons of \hat{q} extracted from measurements at RHIC and from cold nuclear matter experiments, e.g. HERMES, show a large increase of the quenching power at RHIC [30].

The handwaving arguments above can be backed up by calculations which compute energy loss under certain simplifying assumptions. The most important models based on perturbative QCD are

- the Higher Twist (HT) formalism by Guo and Wang [31,32,30]. It uses results from a rigorous calculation of medium-modified fragmentation functions in semi-inclusive deep-inelastic electron scattering off nuclei ($e+A$) and transfers these fragmentation functions to nuclear collisions.
- the AMY formalism based on a series of papers by Arnold, Moore and Yaffe [33,34]. These authors use hard thermal loop resummed perturbation theory, valid at asymptotically large temperatures, to calculate the rate of energy loss for fast partons
- the ASW formalism developed by Armesto, Salgado and Wiedemann [35,36]. Here multiple soft gluon emission is resummed using a Poisson statistics for the number of gluons emitted.
- The GLV approach by Gyulassy, Levai and Vitev [37–39]. They discuss scatterings off static scattering centers in an opacity expansion in the medium.

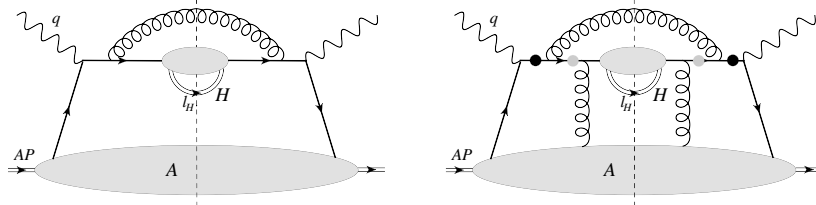


Figure 3. Left panel: diagram contributing to the DGLAP evolution equation of (vacuum) fragmentation functions in semi-exclusive deep-inelastic scattering. Right panel: typical diagram contributing to the modified evolution equations at the twist-4 level. The outgoing parton scatters off the medium and radiates.

As an example we briefly highlight some fundamental ideas of the Higher Twist formalism. Fig. 3 shows typical diagrams contributing to the usual DGLAP equations for fragmentation functions (left panel), and to a set of modified evolution equations that are formally of higher twist in deep-inelastic scattering (DIS). Higher twist in factorized perturbation theory usually refers to sub-leading contributions that are suppressed by powers of the ratio of the non-perturbative over the large perturbative scale, $\sim \Lambda^2/Q^2 \ll 1$. In nuclei, some of those higher twist contributions are re-enhanced through a size factor, such that they enter at a level $L\Lambda^3/Q^2 \sim 1$. Note that we have indicated two propagators each in amplitude and complex conjugated amplitude in the right panel through grey and black circles. The interference between the poles of two of those propagators leads to the LPM suppression effect in the Higher Twist formalism. The modified evolution equations define medium-modified fragmentation functions $\tilde{D}(z)$ which describe the energy loss of partons in semi-exclusive DIS. In their simplest form they can be parameterized as

$$\tilde{D}(z, Q) = \frac{1}{1 - \Delta z} D\left(\frac{z}{1 - \Delta z}\right). \quad (5)$$

where z is the momentum fraction of the hadron within the fragmenting parton and Δz is the average shift due to induced radiation. Similar fragmentation functions, with the average energy loss scaled up to fit the data, can then be used to describe high- P_T data at RHIC.

The energy loss models described above differ in some of their underlying assumptions and are by no means completely equivalent. Nevertheless, all of them manage to describe both the P_T -dependence and the impact parameter-dependence of R_{AA} measured at RHIC remarkably well after *one* parameter, typically \hat{q} or a related quantity, is fixed. With the advent of data on hadron correlations at high P_T additional non-trivial restrictions on fits were available. Typically experiments measure pairs of hadrons, a trigger hadron t and an associated hadron a which are then presented as a per-trigger yield

$$Y(P_t, P_a, \Delta\phi) = \frac{dN/dP_t dP_a d(\Delta\phi)}{dN/dP_t} \quad (6)$$

as a function of the transverse momenta of the trigger and associate particle, P_t and P_a resp., and the relative azimuthal angle $\Delta\phi$. To determine the suppression relative to free proton-proton collisions we can once more look at the appropriate nuclear modification factor

$$I_{AA} = \frac{Y^{AA}(P_t, P_a, \Delta\phi)}{Y^{pp}(P_t, P_a, \Delta\phi)}. \quad (7)$$

I_{AA} poses the first true challenge for jet quenching models, and some studies have found incompatible values of \hat{q} from separate fits to R_{AA} and I_{AA} . It has also become clear that there is a long list of uncertainties, e.g. details of the modeling of the background fireball [40], the treatment of energy loss at early times before the formation of equilibrated quark gluon plasma, etc. [41].

Where do we stand with hard probes? A comparative study by Bass et al. [42] found unacceptably large discrepancies between values of \hat{q} derived from different jet quenching models fitted to RHIC data. The extreme values found in this study are

$$\hat{q} = 18.5 \text{ GeV}^2/\text{fm for ASW}, \quad \hat{q} = 4.5 \text{ GeV}^2/\text{fm for HT}. \quad (8)$$

The good news is that these values are, by far, larger than for cold nuclear matter. However, they are not compatible among each other. A sustained effort is now underway, spear-headed by the TECHQM initiative and the JET collaboration, to systematically investigate hard probes, by comparing and vetting different calculations, and by identifying and narrowing down the sources of theoretical uncertainties.

Once a reliable value of \hat{q} is established, a comparison with its perturbative value in an equilibrated plasma $\hat{q}_{\text{pert}} = 2\epsilon^{3/4}$ will tell us whether the coupling of jets of the quark gluon plasma is weak or strong. Some other interesting developments are the emergence of simulations for the full evolution of jet showers in a medium [43,44], medium modifications to jet shapes [45], and hadron chemistry at large momentum P_T [46].

5. Photons

Hadrons from the bulk carry information from the point of their last interaction (the freeze-out), and hadrons at large momentum P_T carry some information of the fireball integrated

over its history. On the other hand electromagnetic probes, i.e. real and virtual photons (dileptons) have the wonderful property that they do not re-interact once created, due to their large mean-free path in quark gluon plasma. Hence they are unique penetrating probes that can give us unobstructed information about the center of the fireball in nuclear collisions, and about the earliest times during the collision. The following sources of photons are important in relativistic heavy ion collisions [47].

- Prompt hard photons from hard collisions: they are created from annihilation and Compton scatterings, $q + \bar{q} \rightarrow \gamma + g$ and $q + g \rightarrow \gamma + q$ resp., of large momentum partons in the original nuclear wave functions. They dominate the direct photon spectrum at the largest transverse momenta P_T . They also do not carry information about the quark gluon plasma formed, but exhibit some of the initial state effects (shadowing, Cronin effect) mentioned above.
- Fragmentation photons from vacuum bremsstrahlung: any initial hard scattering of partons can lead to bremsstrahlung. Most of the time this will be gluon radiation, but there is a sizable contribution of photons which can be described by parton-to-photon fragmentation functions. Vacuum fragmentation photons have a somewhat steeper P_T -spectrum but are comparable in yield with prompt hard photons except for the largest momenta. Their yield can be modified in nuclear collisions as partons travel over some distance and lose energy before radiating a photon.
- Photons from jet conversions and induced bremsstrahlung [48–51]: as leading jet partons travel through the medium and lose energy through induced gluon radiation, again part of this induced radiation can be in the form of photons. In addition, elastic annihilation and Compton scatterings of fast jet partons with partons in the quark gluon plasma can lead to an effective conversion in which all of the momentum of the fast parton can be transferred to the photon. These processes give competitive photon yields in heavy ion collisions at RHIC and LHC at intermediate P_T of a few GeV/c. The photons carry the full time evolution of the quark gluon plasma fireball as the local conversion rates are proportional to $T^2 \ln T$ and thus one can estimate plasma temperatures T from their yields.
- Thermal photons from both the QGP and the hadronic phase [52,53]: annihilation and Compton as well as bremsstrahlung processes between quarks and gluons also play out in the equilibrated plasma, providing an exponential photon spectrum that dominates at low P_T . Its slope obviously provides the temperature T , although the photons seen in the detector are integrated over the spatial profile as well as the time evolution of the fireball. The hot hadronic gas phase below the phase transition temperature also leads to thermal photons at lower temperatures.

All of these sources have been computed in a sustained effort over two decades. A modern, comprehensive calculation and comparison with data can be found in publications of the McGill group [54]. They compare well with the experimentally measured spectra and R_{AA} of direct photons (decay photons of hadrons like the π^0 bury the direct photon signal in experimental data and have to be subtracted). At low P_T there is ample evidence that the “glow” of the quark gluon plasma has been found and that the temperatures are above the predicted values of T_c . Constraints on other sources, like the conversion photons, are not as stringent. Other observables have been suggested to explicitly find those photons, and

to get a complementary picture of both the medium and jet quenching: e.g. the azimuthal asymmetry v_2 of photons, and photon-hadron correlations.

v_2 is the second order harmonic of the spectrum $dN/d\phi$ w.r.t. the azimuthal angle around the beam axis. The reference axis ($\phi = 0$) is given by the reaction plane. So far we have not discussed v_2 for hadrons from the bulk fireball or for hadrons from jets. In both cases v_2 is positive, meaning more particles are emitted into the reaction plane than out of it. For bulk particles this comes from the hydrodynamic expansion with larger pressure gradients and hence larger flow into the plane, for high- P_T particles it derives from a smaller opacity and less absorption into the plane. It has been predicted in [55] that more conversion photons should be emitted in the elongated direction of the fireball, out of the reaction plane than into the reaction plane. This would lead to a negative v_2 for this photon source, the first process discovered to exhibit this behavior. Its experimental discovery would unanimously confirm conversion and induced bremsstrahlung of jets in medium. Since other photon sources come with vanishing or positive v_2 the sign of the total direct photon v_2 is rather unclear and the absolute value is small due to the cancellations. Experimental data confirm small absolute values but the error bars in the P_T region of interest are too small to pin down the sign [55,56].

One of the most exciting tools in our arsenal combine properties of hard and electromagnetic probes. These are photon-hadron correlations at high momentum. Photon-triggered fragmentation functions can give unprecedented access to the mechanisms of energy loss, as prompt hard photons carry the information about the *initial* momentum of the hard recoil quark or gluon. This information is not available if R_{AA} is considered and it is considerably washed out even if I_{AA} is considered. First experimental results of photon-triggered fragmentation functions are available.

6. Summary

The processes unfolding in collisions of nuclei at high energies are qualitatively understood. The system goes from a phase of strong initial gluon fields through a thermalization process to a hydrodynamically expanding quark gluon plasma which eventually hadronizes. QCD jets, high- P_T hadrons and photons can serve as built-in probes of the new phases of QCD. The field is now moving into a stage of quantitative analysis in which transport coefficients and other observables should be extracted with much reduced error bars. In the near future the high energy ion program at LHC and the future FAIR facility will provide completely new perspectives on the QCD phase diagram.

Acknowledgments

R. J. F. is supported by CAREER Award PHY-0847538 from the U. S. National Science Foundation, RIKEN/BNL Research Center, and DOE grant DE-AC02-98CH10886. He would like to express his gratitude to the organizers of ISNP 2009 for their hospitality and kind invitation.

References

- [1] K. Adcox *et al.* [PHENIX Collaboration], Nucl. Phys. A **757**, 184 (2005).
- [2] J. Adams *et al.* [STAR Collaboration], Nucl. Phys. A **757**, 102 (2005).
- [3] P. F. Kolb and U. W. Heinz, in *Quark Gluon Plasma 3*, ed. R. C. Hwa *et al.*, World Scientific (2003), preprint nucl-th/0305084.
- [4] M. Cheng *et al.*, Phys. Rev. D **77**, 014511 (2008).
- [5] A. Mocsy and P. Petreczky, Phys. Rev. D **73**, 074007 (2006).
- [6] M. Gyulassy and L. McLerran, Nucl. Phys. A **750**, 30 (2005).
- [7] J. D. Bjorken, preprint FERMILAB-PUB-82-059-THY (1982).
- [8] R. S. Bhalerao, Pramana, *to appear*, arXiv:1003.3293 [nucl-th].
- [9] L. D. McLerran and R. Venugopalan, Phys. Rev. D **49**, 3352 (1994).
- [10] L. D. McLerran and R. Venugopalan, Phys. Rev. D **49**, 2233 (1994).
- [11] A. Kovner, L. D. McLerran and H. Weigert, Phys. Rev. D **52**, 6231 (1995).
- [12] F. Gelis, E. Iancu, J. Jalilian-Marian and R. Venugopalan, arXiv:1002.0333 [hep-ph].
- [13] T. Lappi, arXiv:1003.1852 [hep-ph].
- [14] R. J. Fries, J. I. Kapusta and Y. Li, arXiv:nucl-th/0604054.
- [15] T. Lappi and L. McLerran, Nucl. Phys. A **772**, 200 (2006).
- [16] R. Baier, A. H. Mueller, D. Schiff and D. T. Son, Phys. Lett. B **502**, 51 (2001).
- [17] Z. Xu and C. Greiner, Phys. Rev. C **76**, 024911 (2007).
- [18] S. Mrowczynski, Acta Phys. Polon. B **37**, 427 (2006).
- [19] A. Dumitru, Y. Nara and M. Strickland, Phys. Rev. D **75**, 025016 (2007).
- [20] R. J. Fries, B. Muller and A. Schafer, Phys. Rev. C **79**, 034904 (2009).
- [21] R. J. Fries, T. Kunihiro, B. Muller, A. Ohnishi and A. Schafer, Nucl. Phys. A **830**, 519C (2009).
- [22] S. Gavin, L. McLerran and G. Moschelli, Phys. Rev. C **79**, 051902 (2009).
- [23] D. E. Kharzeev, L. D. McLerran and H. J. Warringa, Nucl. Phys. A **803**, 227 (2008).
- [24] Y. Aoki, Z. Fodor, S. D. Katz and K. K. Szabo, Phys. Lett. B **643**, 46 (2006).
- [25] M. Cheng *et al.*, Phys. Rev. D **74**, 054507 (2006).
- [26] M. Laine and Y. Schroder, Phys. Rev. D **73**, 085009 (2006).
- [27] J. W. Cronin, H. J. Frisch, M. J. Shochet, J. P. Boymond, R. Mermod, P. A. Piroué and R. L. Sumner, Phys. Rev. D **11**, 3105 (1975)
- [28] L. D. Landau and I. Pomeranchuk, Dokl. Akad. Nauk Ser. Fiz. **92**, 535 (1953)
- [29] A. B. Migdal, Phys. Rev. **103**, 1811 (1956)
- [30] E. Wang and X. N. Wang, Phys. Rev. Lett. **89**, 162301 (2002).
- [31] X. F. Guo and X. N. Wang, Phys. Rev. Lett. **85**, 3591 (2000).
- [32] X. N. Wang and X. F. Guo, Nucl. Phys. A **696**, 788 (2001).
- [33] P. B. Arnold, G. D. Moore and L. G. Yaffe, JHEP **02060302002**.
- [34] S. Jeon and G. D. Moore, Phys. Rev. C **71**, 034901 (2005).
- [35] C. A. Salgado and U. A. Wiedemann, Phys. Rev. Lett. **89**, 092303 (2002).
- [36] C. A. Salgado and U. A. Wiedemann, Phys. Rev. D **68**, 014008 (2003).
- [37] M. Gyulassy, P. Levai and I. Vitev, Nucl. Phys. B **571**, 197 (2000).
- [38] M. Gyulassy, P. Levai and I. Vitev, Phys. Rev. Lett. **85**, 5535 (2000).
- [39] M. Gyulassy, P. Levai and I. Vitev, Nucl. Phys. B **594**, 371 (2001).
- [40] R. Rodriguez, R. J. Fries and E. Ramirez, preprint
- [41] N. Armesto, M. Cacciari, T. Hirano, J. L. Nagle and C. A. Salgado, J. Phys. G **37**, 025104 (2010).
- [42] S. A. Bass, C. Gale, A. Majumder, C. Nonaka, G. Y. Qin, T. Renk and J. Ruppert, Phys. Rev. C **79**, 024901 (2009).
- [43] N. Armesto, L. Cunqueiro and C. A. Salgado, Eur. Phys. J. C **63**, 679 (2009).
- [44] K. Zapp, G. Ingelman, J. Rathsman, J. Stachel and U. A. Wiedemann, Eur. Phys. J. C **60**, 617 (2009).
- [45] I. Vitev, S. Wicks and B. W. Zhang, JHEP **0811**, 093 (2008).

- [46] W. Liu and R. J. Fries, Phys. Rev. C **77**, 054902 (2008).
- [47] C. Gale, T. C. Awes, R. J. Fries and D. K. Srivastava, J. Phys. G **30**, S1013 (2004).
- [48] R. J. Fries, B. Muller and D. K. Srivastava, Phys. Rev. Lett. **90**, 132301(2003).
- [49] R. J. Fries, B. Muller and D. K. Srivastava, Phys. Rev. C **72**, 041902(2005).
- [50] B. G. Zakharov, JETP Lett. **63**9521996.
- [51] A. Majumder, R. J. Fries and B. Muller, Phys. Rev. C **77**, 065209 (2008).
- [52] J. I. Kapusta, P. Lichard and D. Seibert, Phys. Rev. D **44**, 2774 (1991), *Erratum-ibid.* **47**, 4171 (1993)
- [53] P. B. Arnold, G. D. Moore and L. G. Yaffe, JHEP **0111**0572001.
- [54] G. Y. Qin, J. Ruppert, C. Gale, S. Jeon and G. D. Moore, Phys. Rev. C **80**, 054909 (2009).
- [55] S. Turbide, C. Gale and R. J. Fries, Phys. Rev. Lett. **96**, 032303 (2006).
- [56] R. Chatterjee and D. K. Srivastava, Phys. Rev. C **79**, 021901(2009).